

Second-law Analysis of Solar Chimney Power Plants

Atit Koonsrisuk*

School of Mechanical Engineering, Institute of Engineering, Suranaree University of Technology,
Muang District, Nakhon Ratchasima 30000

*Corresponding Author: atit@sut.ac.th, tel.: 044 224 515, fax.: 044 224 613

Abstract

In order to assess the maximum useful power of solar chimney power plants, a second-law analysis was performed in the present study. The entropy generation number and second-law efficiency for solar chimney power plants are proposed in this study. A comparison is made between the conventional solar chimney power plant (CSCPP) and the sloped solar chimney power plant (SSCPP). Calculations carried out for a wide range of operating conditions show that there is the optimum collector size that provides the minimum entropy generation and the maximum second-law efficiency. It is shown that the second-law efficiency of both systems increases with increasing the system height. It is further shown that SSCPP is thermodynamically better than CSCPP for some configurations.

Keywords: Solar chimney power plant; Sloped solar chimney power plant; Entropy generation; Second-law efficiency; Thermodynamic analysis.

1. Introduction

The solar chimney power plant is a renewable technology for generating electricity from solar energy. It consists of 3 main parts: a solar collector, a turbo generator and a chimney as shown in Fig. 1. Conventionally, the solar collector is a structure with a relatively horizontal roof made from a translucent material. The solar collector serves to convert solar energy coming through the roof into thermal energy of air underneath the roof. As the roof is open at its periphery, buoyancy drives a continuous flow from the roof perimeter into the chimney located at the middle of the roof. This creates a strong air updraft that drives the turbo generator located at the chimney base.

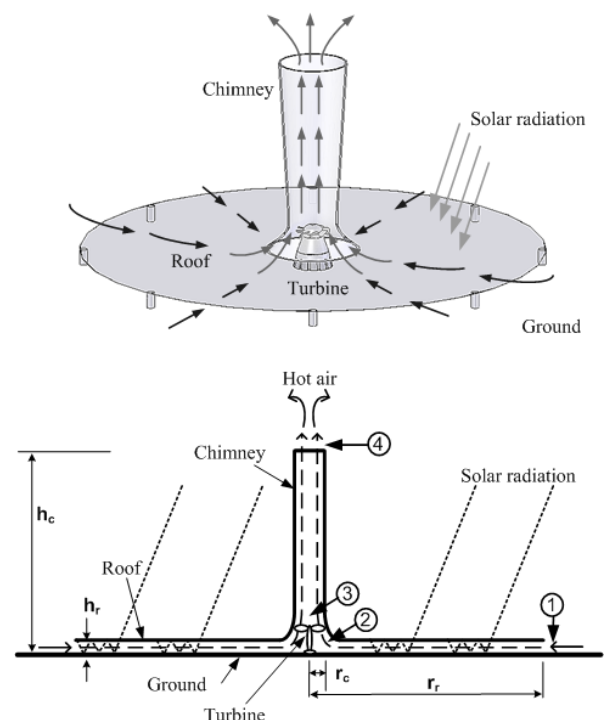


Figure 1 Schematic layout of conventional solar chimney power plant.

TSF-1004

A 50-kW pilot plant of solar chimney power plant was built in Manzanares, Spain (Haaf, 1984). The experimental results indicated that the solar chimney concept is technically viable. However, it was found that its overall thermal efficiency is less than 0.1 percent (Koonsrisuk and Chitsomboon, 2009). To overcome the disadvantage of low efficiency, only large-scaled plants, in which the chimney heights are 1,000 m or more, were proposed in the literature (Lorente et al., 2010). This leads to a very high cost that discourages investment. In order to reduce the construction cost, several researchers proposed the non-conventional concepts in the literature (Bilgen and Rheault, 2005; Kashiwa and Kashiwa, 2008; Koonsrisuk, 2012; Papageorgiou, 2010; Zhou and Yang, 2009; Zhou et al., 2009a, 2009b). Still the construction costs of them are very high. To make this technology economically viable, it requires the performance improvement of the system. The highly efficient smaller plant would encourage investment.

Second law analysis is widely gaining acceptance over traditional energy methods to be a powerful tool for measuring the performance of the power generation systems (Butcher and Reddy, 2007; Dai, 2009; Dincer, 2002; Ganapathy et al., 2009; Hepbasli, 2008; Kaushik et al., 2000; Petela, 2009; Smith and Few, 2001). Unlike the traditional analysis based on the first law analysis, the second law analysis identifies the causes and locations of the thermodynamic inefficiencies in the system, and thus indicates the possibilities of thermodynamic improvement.

This paper deals with the comparison of conventional solar chimney power plants (CSCPP) and sloped solar chimney power plants

(SSCPP) (see the schematic diagram of SSCPP in Fig. 2) by means of second law analysis. The simple-but-accurate mathematical models for CSCPP proposed by Koonsrisuk and Chitsomboon (2012) and for SSCPP proposed by Koonsrisuk (2012) are adopted here to evaluate the flow properties of both systems. Then the entropy generations are computed for various configurations. The results obtained here are expected to provide information that will assist in improving the overall efficiency of the solar chimney power plant and comparing the performance of CSCPP and SSCPP.

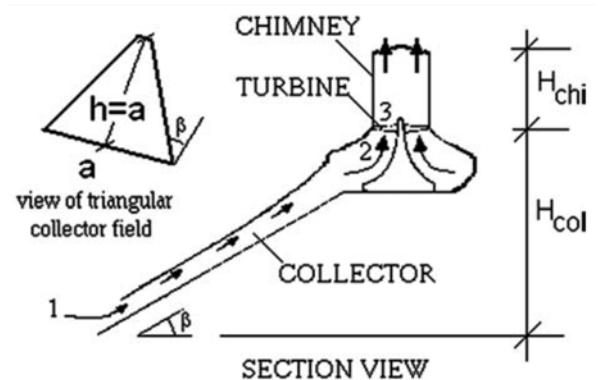


Figure 2 Schematic layout of sloped solar chimney power plant (taken from Bilgen and Rheault (2005)).

2. Mathematical Model

In order to evaluate the entropy generation associated with the energy conversion processes, the relevant flow properties are computed. Those flow properties are evaluated using the mathematical models proposed by Koonsrisuk and Chitsomboon (2012) for CSCPP and the one proposed by Koonsrisuk (2012) for SSCPP. Then the entropy generation number and second-law efficiency are computed. The equations to compute them are as follows:

TSF-1004

2.1 Mathematical model for CSCPP

Koonsrisuk and Chitsomboon (2012) proposed to use the system of equations as follows:

$$\int_{col} dp = \frac{\dot{m}^2}{\rho_{ave,col}} \int \frac{dA}{A^3} - \frac{\dot{m}q''}{\rho_{ave,col}c_p T_{ave,col}} \int \frac{dA_r}{A^2} + \frac{1}{2} f \frac{\dot{m}^2}{\rho_{ave,col}} \int \frac{dr}{A^2 h_{roof}} \quad (1)$$

$$T_2 = T_1 - \frac{\dot{m}^2}{2c_p \rho_{ave,col}^2} \left(\frac{1}{A_2^2} - \frac{1}{A_1^2} \right) + \frac{q'' A_r}{c_p \dot{m}} \quad (2)$$

$$T_3 = T_2 \left(\frac{p_3}{p_2} \right)^{\frac{\gamma-1}{\gamma}} \quad (3)$$

$$p_3 = p_4 + \frac{1}{2} (\rho_3 + \rho_4) \cdot g \cdot h_c + f \frac{\dot{m}^2}{2(\rho_3 + \rho_4) \pi^2 r_c^5} h_c \quad (4)$$

$$T_4 = T_3 - \frac{g}{c_p} h_c \quad (5)$$

$$\rho_2 = \frac{p_2}{RT_2}, \rho_3 = \frac{p_3}{RT_3}, \rho_4 = \frac{p_4}{RT_4} \quad (6)$$

$$\dot{W}_{ext} = \frac{\dot{m}}{(\rho_2 + \rho_3)/2} (p_2 - p_3) \quad (7)$$

Please be noted that Eqs. (1) and (4) are modified from the original ones. They are added the terms for pressure drop due to friction. Koonsrisuk (2012) defined the ratio between the collector inlet area and the collector outlet area as AR12 ($AR12 = A_1/A_2$) and using $AR12 = 2$ in

the study. In order to obtain the system with $AR12 = 2$, the roof height of the collector must be varies linearly from the collector inlet to the collector outlet. Let assume that

$$h_{roof} = b(r + d) \quad (8)$$

where b and d are the constants and r is the coordinate in the direction of roof radius.

2.2 Mathematical model for SSCPP

Koonsrisuk (2012) proposed to use the system of equations as follows:

$$\int_{col} dp = -\rho_{ave,col} g \int dz + \frac{\dot{m}^2}{\rho_{ave,col}} \int \frac{dA}{A^3} - \frac{\dot{m}q''}{\rho_{ave,col}c_p T_{ave,col}} \int \frac{dA_r}{A^2} + \frac{1}{2} f \frac{\dot{m}^2}{\rho_{ave,col}} \int \frac{dr}{A^2 h_{roof}} \quad (9)$$

$$T_2 = T_1 - \frac{\dot{m}^2}{2c_p \rho^2} \left(\frac{1}{A_2^2} - \frac{1}{A_1^2} \right) - \frac{gh_{col}}{c_p} + \frac{q'' A_r}{c_p \dot{m}} \quad (10)$$

$$T_3 = T_2 \left(\frac{p_3}{p_2} \right)^{\frac{\gamma-1}{\gamma}} \quad (11)$$

$$p_3 = p_4 + \frac{1}{2} (\rho_3 + \rho_4) \cdot g \cdot h_c + f \frac{\dot{m}^2}{2(\rho_3 + \rho_4) \pi^2 r_c^5} h_c \quad (12)$$

$$T_4 = T_3 - \frac{g}{c_p} h_c \quad (13)$$

TSF-1004

$$\rho_2 = \frac{P_2}{RT_2}, \rho_3 = \frac{P_3}{RT_3}, \rho_4 = \frac{P_4}{RT_4} \quad (14)$$

$$\dot{W}_{\text{ext}} = \frac{\dot{m}}{(\rho_2 + \rho_3)/2} (p_2 - p_3) \quad (15)$$

Please be noted that Eqs. (9) and (12) are modified from the original ones. They are added the terms for pressure drop due to friction. In addition, Koonsrisuk (2012) used the relation

$$q'' = \eta_{\text{col}} I \quad (16)$$

where the value of $\eta_{\text{col}} = 0.56$ was assumed.

2.3 Entropy generation number

In this study, the entropy generation of a system undergoing a change from an initial state to a final state is defined as (Bejan, 2006)

$$\begin{aligned} S_{\text{gen}} &= S_f - S_i \\ &= \dot{m} \left(c_p \ln \frac{T_f}{T_i} - R \ln \frac{p_f}{p_i} \right) \end{aligned} \quad (17)$$

In order to evaluate the irreversibility loss in heat exchangers, Bejan (1982) defined the entropy generation number as

$$N_s = \frac{S_{\text{gen}}}{\dot{m} c_p \Delta T} \quad (18)$$

Multiplying both the numerator and denominator by ΔT (the temperature difference between ambient and collector outlet) yields

$$N_s = \frac{S_{\text{gen}} \Delta T}{\dot{m} c_p \Delta T}$$

If we assume that $\dot{m} c_p \Delta T = q'' A_r$, then N_s can be interpreted as the entropy generated per unit amount of useful solar heat gain multiplied by the temperature change across the collector. However, Eqs. (2) and (10) show that $\dot{m} c_p \Delta T$ is not exactly equal to $q'' A_r$. Order of magnitude analysis reveals that $\dot{m} c_p \Delta T$ is approximately

equal to $q'' A_r$ for CSCPP. On the other hand, the magnitude of the term $g h_{\text{col}} / c_p$ in Eq. (10) is relatively high. As a result, $\dot{m} c_p \Delta T$ differs significantly from $q'' A_r$ for SSCPP. Consequently, we propose the entropy generation number for solar chimney power plants as

$$N'_s = \frac{S_{\text{gen}} \Delta T}{q'' A_r} \quad (19)$$

2.4 Second-law efficiency

Generally, we defined the efficiency of solar chimney power plants on the basis of the first law of thermodynamics as

$$\eta_I = 100 \times \frac{\dot{W}_{\text{ext}}}{I \times A_r} \quad (20)$$

It will be shown later that η_I of all tested cases are about 1 percent. This leads to the impression that the solar chimney power plant is not worth the investment. The judgment based on the above definition may be not fair because the input energy of this technology is free and renewable. To assess the effectiveness of energy resource utilization, we define the second-law efficiency for the solar chimney power plant as

$$\eta_{II} = 100 \times \frac{\dot{W}_{\text{ext}}}{\dot{W}_{\text{rev}}} \quad (21)$$

where the reversible work of a system is defined as (Bejan, 2006)

$$\begin{aligned} \dot{W}_{\text{rev}} &= \dot{m} \left(c_p (T_1 - T_4) + T_1 (S_4 - S_1) \right. \\ &\quad \left. + \frac{1}{2} (V_1^2 - V_4^2) - g (h_c + h_{\text{col}}) \right) \\ &\quad + \left(1 - \frac{T_1}{T_{\text{ave,col}}} \right) q'' A_r \end{aligned} \quad (22)$$

TSF-1004

3. Description of the tested cases

The CSCPP and SSCPP studied here have a power capacity of 5 MW. Their geometric dimensions and operating conditions are adopted from Bilgen and Rheault (2005) as shown in Table 1. In addition, the wall friction factor is set to $f = 0.008428$ (Zhou et al., 2009) for all tested cases.

Table 1 Design parameters for 5 MW CSCPP and SSCPP

Parameters	CSPPP	SSCPP
A_r (m ²)	950,000	950,000
h_{col} (m)	-	848
r_c (m)	27	27
h_c (m)	547	123
T_1 (K)	293	293
p_1 (Pa)	101,325	101,325
I (W/m ²)	1,000	1,000

According to the formulations described in Section 3, the MATLAB code was developed. The systems of equations are solved by using Newton-Raphson method. The iterative scheme starts with an initial guess of the values of the unknowns. The process is continued until the unknowns do not change from one iteration to the next, within a specified convergence criterion of 1×10^{-5} (Koonsrisuk, 2012; Koonsrisuk and Chitsomboon, 2012).

4. Results and Discussion

4.1 Effects of A_r

The collector area was varying to investigate its effects on N_s , N'_s , η_I and η_{II} and the results are shown in Figs. 3 and 4. Figure 3

shows that N_s of SSCPP and CSCPP do not differ significantly. On the other hand, N'_s of SSCPP is significantly lower than that of CSCPP. This is due to the fact that ΔT of CSCPP is higher than that of SSCPP and the entropy generation increases with the temperature difference. According to these findings, using N_s to characterize solar chimney power plants could be misleading and using N'_s would be more appropriate. The reason of lower ΔT in SSCPP is that the air temperature is reduced due to the elevation change through the collector as represented by the term gh_{col}/c_p in Eq. (10). Equation (10) describes that the temperature in the collector of SSCPP decreases due to the kinetic energy change (the second RHS term) and the effect of temperature drop with altitude (the third RHS term), and increases due to the solar heat gain (the fourth RHS term). The magnitude of each terms are shown in Table 2. The values shown are the average when the collector area varied from 500,000 to 1,200,000 m². It should be noted that $\dot{m}c_p\Delta T$ is approximately equal to $q''A_r$ for CSCPP and the temperature change due to elevation change through the collector is relatively significant for SSCPP as discussed previously.

Table 2 Average values of temperature changes

Terms	CSCPP	SSCPP
ΔT (K)	+12.34	+3.83
$\Delta T_{q''}$ (K)	+12.42	+12.15
ΔT_{AR12} (K)	-0.07	-0.06
ΔT_{hcol} (K)	-	-8.27

TSF-1004

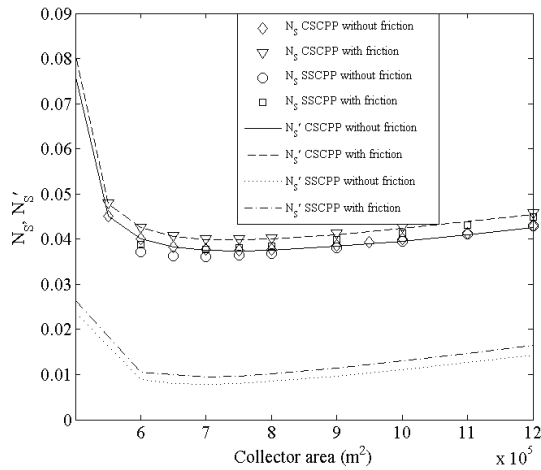


Figure 3 Influence of collector area and friction losses on N_s and N'_s .

In could be seen from Fig. 3 that the friction losses do not have much effect on the entropy generation number. Equation (1) shows that the pressure change across the collector increases due to heat addition (the second RHS term), and it decreases due to flow area reduction toward the roof center (the first RHS term) and also due to friction loss (the third RHS term). Table 3 shows the significance of these three effects including the pressure drop caused by friction through the chimney. According to Table 3, the pressure drop due to flow area change through the collector is relatively significant and the pressure losses due to friction have only a minor effect that we could neglect them. This is in accordance with Koonsrisuk et al. (2010), although we used different relations to predict the pressure loss terms.

The first-law and second-law efficiencies are illustrated in Fig. 4. Obviously, both η_I and η_{II} of SSCPP are higher than those of CSCPP. As mentioned previously, the values of η_I for both types are about 1 percent. However, the average value of η_{II} for SSCPP is about 80 percent while

it is about 40 percent for CSCPP. In other words, SSCPP is converting 80 percent of the available work potential to useful work and it is only 40 percent for CSCPP. In addition, it can be seen that the influence of friction on η_{II} increases with A_c .

Table 3 Average percentage values of pressure changes

Terms	CSCPP	SSCPP
$100 \times \Delta p_{q^*} / (p_2 - p_3)$	0.57	0.28
$100 \times \Delta p_{A12} / (p_2 - p_3)$	79.20	40.38
$100 \times \Delta p_{fric,col} / (p_2 - p_3)$	7.40	4.03
$100 \times \Delta p_{fric,c} / (p_2 - p_3)$	9.21	1.16

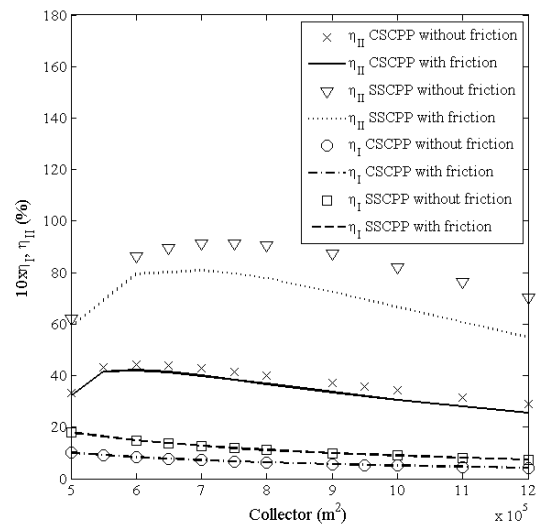


Figure 4 Influence of collector area and friction losses on η_I and η_{II} .

Schlaich (1995) reported that optimal dimensions for a solar chimney do not exist. According to Figs 3 and 4, however, the minimum entropy generation and the maximum second-law efficiency for the given plant both occur when the collector area being 700,000 m².

TSF-1004

4.2 Effects of the system height

The system height of CSCPP equals to h_c , while it is the sum of h_{col} and h_c for SSCPP. The system height for both systems was varied from 500 to 1,000 m. It was found that changing h_{col} or h_c does not affect N_s , N'_s and η_{II} of SSCPP as long as the sum of h_{col} and h_c remains a constant. Figure 5 shows the effects of system height on N_s and N'_s . It is clear that an increase of system height will result in a lower entropy generation number. When the height is less than 700 m, the entropy generation number of CSCPP is less than that of SSCPP and when the height is larger than 700 m, the entropy generation number of CSCPP is larger than that of SSCPP. These patterns also happen with η_{II} in Fig. 6. It is evident that η_{II} increases with the height. In addition, when the height is less than 800 m, η_{II} of CSCPP is larger than that of SSCPP and when the height is larger than 800 m, the η_{II} of CSCPP is less than that of SSCPP.

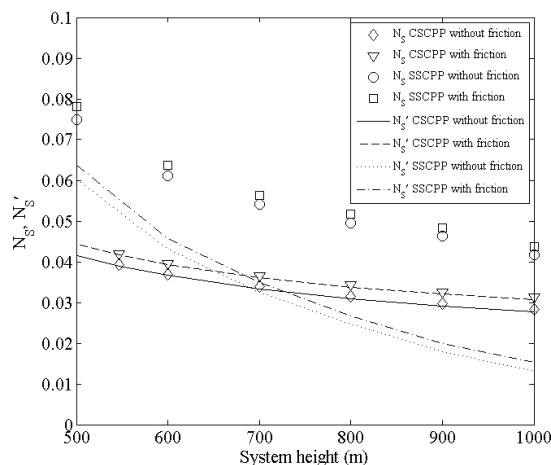


Figure 5 Influence of system height and friction losses on N_s and N'_s .

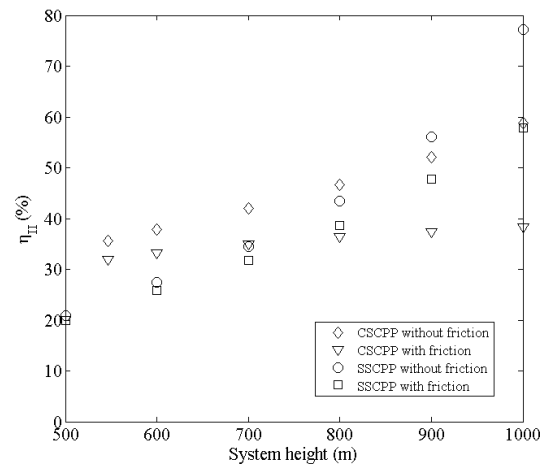


Figure 6 Influence of system height and friction losses on η_{II} .

Based on the board range of studies when the collector area varied from 500,000 to 1,200,000 m^2 , the system height varied from 500 to 1,000 m, AR_{12} from 2 to 500, \dot{W}_{ext} from 0 to 8 MW, and I from 100 to 2,000 W/m^2 , it should be notify that $(S_2 - S_1)/(S_4 - S_1)$ is approximately equal to one and $(S_3 - S_4)/(S_4 - S_1)$ could be neglected. This reveals that most of irreversibilities occur in the collector. In other words, the improvement of collector shape is in need.

5. Conclusion

This paper compares CSCPP and SSCPP using the second law of thermodynamics. In order to examine the entropy generation number and second-law efficiency, the computations based on the mathematical models proposed in the literature were conducted. The appropriate entropy generation number and second-law efficiency for solar chimney power plants are proposed in the study. For the 5-MW plants studied here, it was found that there is the

TSF-1004

optimum collector size that provides the minimum entropy generation and the maximum second-law efficiency. On the other hand, the entropy generation number decreases and the second-law efficiency increases with increasing the system height. Results show that SSCPP is thermodynamically better than CSCPP for some configurations and is thermodynamically inferior for some other configurations. In addition, the study reveals the relative magnitudes of various effects that change pressure and temperature of the system.

6. Acknowledgement

This research was sponsored by the SUT Research and Development fund of Suranaree University of Technology (SUT), Thailand.

7. References

- Bejan, A. (1982). *Entropy generation through heat and fluid flow*, John Wiley & Sons, New York.
- Bejan, A. (2006). *Advanced Engineering Thermodynamics*, 3rd edition, Wiley, New York.
- Bilgen, E., Rheault, J. (2005). Solar chimney power plants for high latitudes, *Solar Energy*, vol.79(5), pp.449-458.
- Butcher, C.J., Reddy, B.V. (2007). Second law analysis of a waste heat recovery based power generation system, *International Journal of Heat and Mass Transfer*, vol.50, pp.2355–2363.
- Dai, Y.P., Wang, J.F., Gao, L. (2009). Exergy analysis, parametric analysis and optimization for a novel combined power and ejector refrigeration cycle, *Applied Thermal Engineering*, vol.29, pp.1983-1990.
- Dincer, I. (2002). Thermal energy storage systems as a key technology in energy conservation, *Int. J. Energy Res.*, vol.26, pp.567-588.
- Ganapathy, T., Alagumurthi, N., Gakkhar, R.P., Murugesan, K. (2009). Exergy analysis of operating lignite fired thermal power plant, *Journal of Engineering Science and Technology Review*, vol.2, pp.123-130.
- Haaf, W. (1984). Solar chimneys: part II: preliminary test results from the Manzanares plant, *International Journal of Solar Energy*, vol.2, pp.141-161.
- Hepbasli, A. (2008). A key review on exergetic analysis and assessment of renewable energy resources for a sustainable future, *Renewable and Sustainable Energy Reviews*, vol.12, pp.593-661.
- Kashiwa, B.A., Kashiwa, C.B. (2008). The solar cyclone: a solar chimney for harvesting atmospheric water, *Energy*, vol.33(2), pp.331-339.
- Kaushik, S.C., Misra, R.D., Singh, N. (2000). Second law analysis of a solar thermal power system, *International Journal of Solar Energy*, vol.20, pp.239-253.
- Koonsrisuk, A. (2012). Mathematical modeling of sloped solar chimney power plants, *Energy*, vol.47(1), pp.582-589.
- Koonsrisuk, A., Chitsomboon, T. (2009). Partial geometric similarity for solar chimney power plant modeling. *Solar Energy*, vol.83(9), pp.1611-1618.
- Koonsrisuk, A., Chitsomboon, T. (2013). Mathematical modeling of solar chimney power plants, *Energy*, vol.47(1), pp.582-589.

TSF-1004

- Koonsrisuk, A., Lorente, S., Bejan, A. (2010). Constructal solar chimney configuration, *International Journal of Heat and Mass Transfer*, vol.53, pp.327-333.
- Lorente, S., Koonsrisuk, A., Bejan, A. (2010). Constructal distribution of solar chimney power plants: few large and many small, *International Journal of Green Energy*, vol.7, pp.577-592.
- Papageorgiou, C. (2010). Floating solar chimney technology, in: Rugescu, R.D. (Ed.), *Solar Energy book of INTECH*.
- Petela, R. (2009). Thermodynamic study of a simplified model of the solar chimney power plant, *Solar Energy*, vol.83, pp.94-107.
- Schlaich, J. (1995). *The Solar Chimney*. Edition Axel Menges: Stuttgart, Germany.
- Smith, M.A., Few, P.C. (2001). Second law analysis of an experimental domestic scale cogeneration plant incorporating a heat pump, *Applied Thermal Engineering*, vol.21, pp.93-110.
- Zhou, X.P., Yang, J.K. (2009). A novel solar thermal power plant with floating chimney stiffened onto a mountainside and potential of the power generation in China's Deserts, *Heat Transfer Engineering*, vol.30(5), pp.400-407.
- Zhou, X.P., Yang, J.K., Wang, F., Xiao, B. (2009a). Economic analysis of power generation from floating solar chimney power plant, *Renewable & Sustainable Energy Reviews*, vol.13(4), pp.736-749.
- Zhou, X.P., Yang, J.K., Wang, J., Xiao, B. (2009b). Novel concept for producing energy integrating a solar collector with a man made mountain hollow, *Energy Conversion and Management*. vol.50(3). pp.847-854.

- Zhou, X.P., Yang, J.K., Xiao, B., Hou, G., Xing, F. (2009). Analysis of chimney height for solar chimney power plant, *Applied Thermal Engineering*. vol.29, pp.178-185.

8. Nomenclature

- A flow area, m²
- AR12 area ratio between positions 1 and 2
- A_r roof area, m²
- b constant (see Eq. (8))
- c_p specific heat capacity at constant pressure, J/(kg.K)
- d constant (see Eq. (8))
- f friction factor
- g gravitational acceleration, m/s²
- h_c chimney height, m
- h_{roof} roof height above the ground, m
- I solar irradiation, W/m²
- \dot{m} mass flow rate, kg/s
- N_s typical entropy generation number
- N'_s entropy generation number for solar chimney power plants
- q'' insolation, W/m²
- p pressure, Pa
- R ideal gas constant, J/kg.K
- RHS Right-hand side
- r coordinate in roof radius direction
- r_c chimney radius, m
- r_r collector radius, m
- S entropy, kJ/K
- S_{gen} entropy generation, kJ/K
- T absolute temperature, K
- V flow velocity, m/s
- \dot{W}_{ext} power extracted by turbine, W
- \dot{W}_{rev} reversible power output, W

TSF-1004

	col	collector
	i	initial state
	f	final state
	fric	friction
	roof	roof
<i>Greek symbols</i>		
Δp		pressure drop, Pa
$\Delta p_{q,r} / (p_2 - p_3)$		ratio between the pressure change due to solar heat addition and the pressure extraction at the turbine, Pa
$\Delta p_{A12} / (p_2 - p_3)$		ratio between the pressure change due to flow area change through the collector and the pressure extraction at the turbine, Pa
$\Delta p_{\text{fric,col}} / (p_2 - p_3)$		ratio between the pressure loss due to friction through the collector and the pressure extraction at the turbine, Pa
$\Delta p_{\text{fric,c}} / (p_2 - p_3)$		ratio between the pressure loss due to friction through the chimney and the pressure extraction at the turbine, Pa
ΔT		temperature difference between ambient and collector outlet, K
$\Delta T_{q,r}$		temperature change due to solar heat addition, K
ΔT_{AR12}		temperature change due to flow area change inside the collector, K
ΔT_{hcol}		temperature change due to elevation change through the collector, K
η_{col}		collector efficiency
η_{I}		first-law efficiency
η_{II}		second-law efficiency
γ		specific heat ratio
ρ		density, kg/m ³

Subscripts

1,2,3,4	position as depicted in Fig. 1
ave	average value
c	chimney